FINITE ELEMENT STUDY OF LAMB WAVE INTERACTIONS WITH HOLES AND THROUGH THICKNESS DEFECTS IN THIN METAL PLATES

G. S. Verdict, P. H. Gien, and C. P. Burger

Department of Mechanical Engineering, Texas A&M University
College Station, Texas 77843-3123

INTRODUCTION

TAP/NDE (Thermo-Acousto-Photonic nondestructive evaluation) has been developed to the point where it is possible to confidently explore many different application areas. One area of interest is the inspection of defects around rivet holes and under rivet heads. This problem is of concern not only from a safety point of view in aging aircraft, but also has major economic implications. For example, a heavy "C" check for a Boeing 707 requires the physical removal, inspection and replacement of many thousands of structural fasteners. Of the various types of rivets the round head rivet hole was chosen for this preliminary analysis (Fig. 1). Since it is not known how Lamb waves interact with an in situ rivet, we have chosen to restrict this analysis to the simplest possible case where there is no rivet in the hole. This corresponds to the current practice of removing the rivet and then using eddy current probes to inspect the hole. Our goal is to develop an inspection technique that does not require the physical removal of the rivet. The buried in-plane defect study was undertaken to provide real time, on-line detection of flaws during the processing of the material to prevent these flaws from causing in-service, premature rivet hole degradation. This inspection would prevent flawed materials from entering service.

The defects chosen for this analysis correspond to certain forms of corrosion cracking that occur in rolled plates. Due to the orientation of the material grain boundaries, intergranular corrosion occurs at the edges of the drilled hole and the free edges of the plate resulting in the kinds of defects depicted in Fig. 2. These types

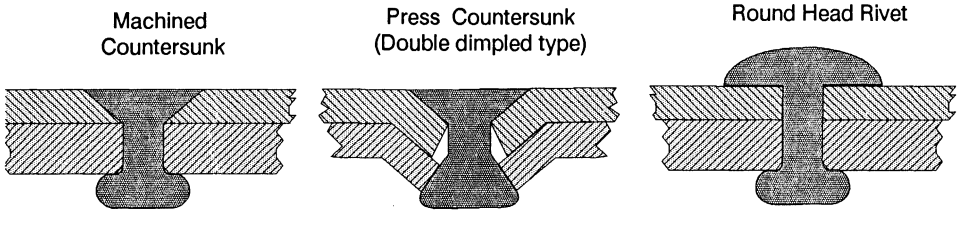

Fig. 1 Common rivet installations

Review of Progress in Quantitative Nondestructive Evaluation, Vol. 11
Edited by D.O. Thompson and D.E. Chimenti, Plenum Press, New York, 1992

of defects are difficult to inspect since they usually lie beneath the rivet head. The diameter for the rivet hole chosen in this study is 0.92 mm. This defect will be referred to as an edge breaking defect. A second type of defect was also studied which was not at the edge of the plate. This defect will be referred to as an in-plane defect. A range of edge breaking defect length values was simulated (zero to 0.762 mm in steps of 0.05 mm) as well as range of location values (from center line to 0.2 mm from free edges in steps of 0.1). The varying length cracks were all located at the center line of the plate. A similar range of in-plane defect locations and lengths were also simulated.

This paper presents a simulation of laser induced Lamb waves interacting with a defect in a rivet hole. The data obtained from these simulations is then used to train neural networks to find and characterize the in-plane location and length of the defect. The simulation is strictly based on the modeling techniques presented in [1] where it was shown that finite element models were able to reproduce the experimentally measured out-of-plane displacements produced by laser generated, zero'th order symmetric and antisymmetric Lamb waves in defect free isotropic materials. For modeling defects, techniques have been developed to reproduce experimental results of laser induced Rayleigh waves interacting with shallow surface breaking defects [2]. This allows us to confidently model the defects in the manner used in this paper. Finally, initial results of FE (finite element) models showing Lamb wave interactions with buried in-plane defects will also be presented.

FINITE ELEMENT MODEL PARAMETERS

The physical situation being modeled is shown in Fig. 3, which is similar to the experimental setup commonly used in TAP/NDE. A complete description of the various elements is given in [3] and [4]. The salient features of the system are a pulsed 300 millijoule Nd:YAG Laser focused to a point, 2 mm in diameter, on the surface being tested. Rapid thermal heating occurs in a thin surface skin which gives rise to Lamb waves in thin plates, and to combined Lamb and Rayleigh waves in specimens thicker than approximately 3 mm depending on the material being tested [5]. In all cases, the incident energy density is well within the thermo-elastic range, i.e., there is no ablation. In TAP/NDE, the preferred technique for receiving signals is through the use of fiber tip interferometry which allows us to measure absolute displacements on the order of a nanometer at a point without contacting the specimen or requiring a coupling medium for the sensor. The FE model simulates this capability by extracting

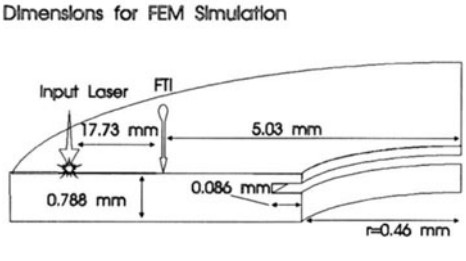

Fig. 2. Defect and source/receiver geometry for simulation.

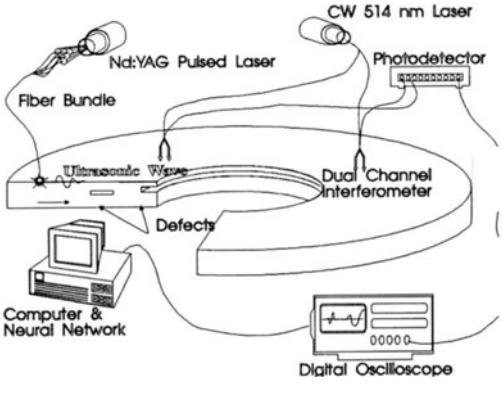

Fig. 3. Typical TAP/NDE layout with rivet hole and defects.

normal displacement time histories at the locations of the fiber tip interferometer (FTI) shown in Fig. 2.

The exact dimensions used in the simulation are reported in Fig. 2. The plate material was 2024-T3 Aluminum, with a Young's modulus of 75 GPa, a Poisson's ratio of 0.33, and a mass density of 2030 kg/m^3. The finite element model consisted of 330 axisymmetric elements and an unconditionally stable direct integration scheme was employed with an integration time step of 0.08 microseconds. The element sizes used throughout the model were 0.1 by 0.1 mm, while a refined mesh of 0.1 by 0.05 mm was used around the immediate area of the defect as shown in Fig. 4. A study showed that the addition of these finer elements did not produce spurious waves when compared to a model with uniform mesh size. Comparisons with experimental studies, [1] and [2], have given us confidence that the model parameters selected for this analysis will yield accurate and valid FE models. The in-plane forcing function used to model the laser source was derived from non-linear thermal diffusion equation simulations and was similar to that described in [1]. The laser generation produces two waves, a zero'th order symmetric Lamb wave traveling approximately twice the speed of a zero'th order antisymmetric Lamb wave. Since both waves emanate from the source, they separate from each other after traveling a suitable distance, which in this case, is approximately 10 mm. It was for this reason that we located the source at 17.7 mm from the point where normal to he surface displacements were extracted from the model, thus ensuring good separation of the various Lamb modes over most of the frequency range of interest. An additional benefit was that the interactions of the two distinct Lamb modes with defects could be observed individually without overlapping and mixing with each other. The disadvantage of this arrangement is that a rather large finite element model cannot be avoided.

LAMB WAVE INTERACTIONS WITH DEFECTS

Fig. 4 shows the results of the simulation as the first distinguishable zero'th order symmetric Lamb wave approaches the defect. This wave was observed to reflect from the defect free edge as a symmetric Lamb wave. In the presence of a defect which was located asymmetrically with respect to the midplane of the plate, the symmetric Lamb wave reflected and mode converted to an antisymmetric Lamb wave. It should be noted that for this and all subsequent figures showing Lamb wave iteractions with defects, the displacements are greatly exaggerated only for ease of visual inspection. For the defect placed symmetrically as shown in Fig. 5, the symmetric Lamb wave re-

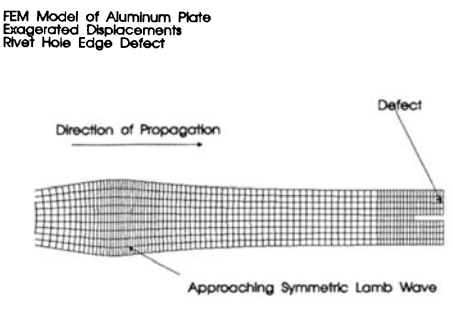

Fig. 4. Simulated symmetric Lamb wave approaching defect.

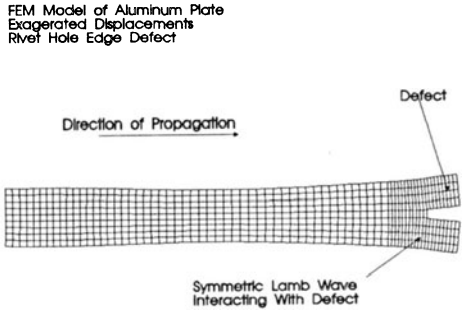

Fig. 5. Symmetric Lamb wave interacting with edge defect.

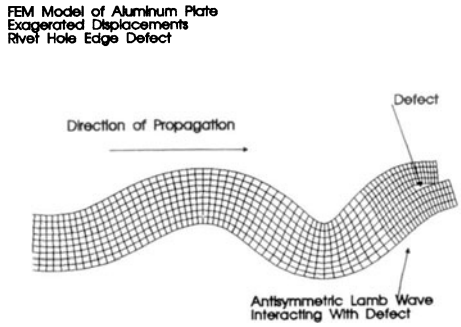

Fig. 6. Asymmetric Lamb wave interacting with defect.

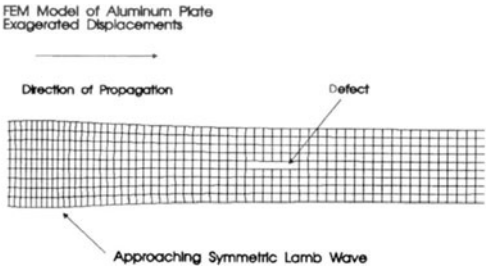

Fig. 7. Symmetric Lamb wave approaching in-plane defect .

flected as a purely symmetric Lamb wave. There was no observed mode conversion from the zero'th order mode to higher order modes, although this effect might be too small to be visually detected in the present simulation. Following closely behind the symmetric Lamb waves was the slower zero'th order antisymmetric Lamb wave shown approaching and interacting with the edge breaking defect in Fig. 6. It was observed that the antisymmetric Lamb wave reflected from the defect free edge as an antisymmetric Lamb wave. In the presence of some edge breaking defects, the frequency content of the reflected wave was altered, but no mode conversion to symmetric or higher order antisymmetric waves was observed. In general, it was observed qualitatively that the deformations around the defect were largely dilational for the case of symmetric Lamb waves, while the antisymmetric waves induced large shear deformations in the material around the defect.

Fig. 7 shows a symmetric Lamb wave approaching an in-plane defect. Fig. 8 shows how this wave interacts and passes over the symmetrically placed defect. The wave reforms on the other side of the defect as a substantially unaltered symmetric Lamb wave. If the defect is placed asymmetrically with respect to the midplane of the plate, then a mode conversion occurs resulting in a transmitted antisymmetric Lamb wave. Again, the predominant deformations in the material around the defect are dilational. Fig. 9 shows an antisymmetric Lamb wave approaching and interacting with a buried

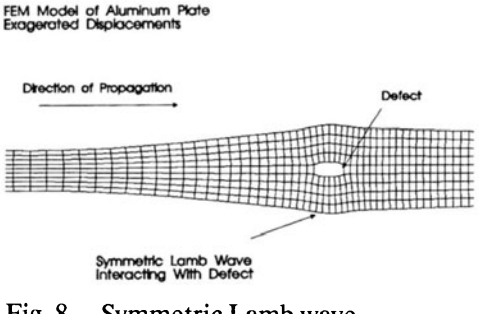

Fig. 8. Symmetric Lamb wave interacting with defect.

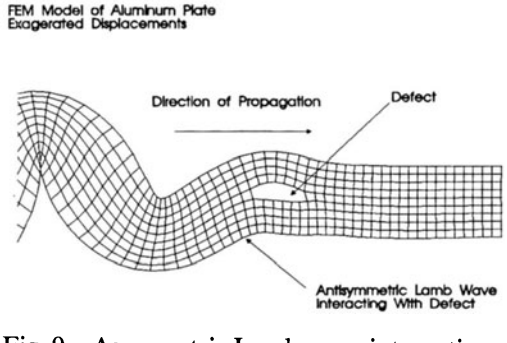

Fig. 9. Asymmetric Lamb wave interacting with defect

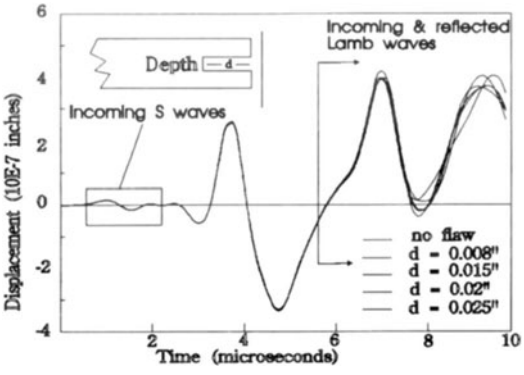

Fig. 10. Out of plane displacement time histories for various depths of defect.

defect. The wave converts into two antisymmetric waves traveling through the thin plate above and below the defect. This substantially alters the shape of the anti-symmetric wave as it recombines on the far side of the defect. Here again, it is to be noted that large shearing deformations are observed in the antisymmetric wave interaction as opposed to the largely dilational deformations observed in the symmetric wave interactions.

NEURAL NETWORK TRAINING DATA

The out-of-plane displacement time histories predicted by the FEM model for various edge breaking defect depths are shown in Fig. 10. Since this is a displacement time history of a point identified as FTI in Fig. 2, it is clear that the arrival of various waves can be clearly identified. For example, the first three peaks of the curve indicate the arrival of the lowest frequency zero'th order symmetric Lamb waves which travel at the highest speed from the point of application of the forcing function. They are followed in succession by the higher frequency symmetric waves, then by the higher frequency anti-symmetric waves and finally by the lower frequency anti-symmetric waves. After approximately six microseconds, the low frequency symmetric Lamb waves have already reflected from the hole edge and are mixing with slower incoming antisymmetric Lamb waves. The different traces shown in Fig. 10 correspond to results of models used to study the effects of different defect depths. It should be clear that a single signal contains both the incoming and reflected waves. Since the differences between signals in Fig. 10 are so small and spread over an indistinguishable range of time, it is not intended that this figure be used to identify individual traces, but rather to show qualitatively that the signals do vary.

The time histories from Fig. 10 were used to train two neural networks. The first network was used to determine the presence of a defect, while the second was used to predict the length and location of a defect. The same training data was used for both networks. The training data was assembled from Fig. 10 by digitizing the signal from $t = 8.5$ microseconds to $t = 12$ microseconds. Before 8.5 microseconds, there was no significant difference in the signals due to the fact that most waves had not reflected off the boundary and returned to the sampling point until 8.5 microseconds. The data was sampled at 24 equally spaced intervals in this time period.

When using neural networks, it is critical that the network should be supplied with enough training cases and data samples so that the network can effectively map the

function which describes the data. In previous studies using FE models to simulate the propagation of Lamb waves, different types of force application schemes enabled the creation of either pure symmetric or antisymmetric Lamb waves or a combination of both like those seen in prior experimental results [1]. Using only four different models for each crack parameter (length and location) for the edge breaking defect study, three scenarios were run for each. Either pure symmetric, antisymmetric, or a combination wave packet was used to interrogate each defect. This approach was taken in order to generate twelve data sets for each defect parameter providing enough training data for the neural network while saving time with the generation and execution of additional models with different defect parameters. Standard FFT's were done on each displacement time history data set. Visual inspection of the FFT's showed significant differences for most cases.

Initially, a fast back-propagation network with twenty-four inputs and two rows of twenty and ten processing elements, respectively, was constructed and tested. This network would determine the length and location of an edge breaking defect. The symmetric, antisymmetric and combination Lamb wave data for each model was fed into the network as a training set. Convergence of this network was slow with the best result of a test case being a root mean square error value of 50% in the network's returned value after eighteen hours of training on an i80386-33 PC. The network was tested at even time intervals up to this point to prevent over-training of the network. At this point, due to excessive errors and lengthy training periods, the whole procedure had to be re-evaluated.

Previous research by this group had shown that a signal very similar to the combination wave packet seen in experiments could be produced by combining pure antisymmetric and symmetric Lamb wave FE models displacement time histories. This procedure was accomplished by determining coefficients for a linear equation which combined these two signals using a minimization of a root mean square function. Here-in lay the answer to our failed first trial. The FFT is based on a linear transformation of a function to the frequency domain. If the antisymmetric and symmetric wave data could be linearly combined to describe the combination wave packet, then information from FFT's of the antisymmetric and symmetric wave data was already contained in the combination wave packet FFT . So instead of providing the neural net with twelve unique training data sets, there were only four unique data sets and the other eight cases contained the same information which was in the four unique data sets. Thus, only four unique training cases were presented to the network and this was apparently not enough data to effectively train the neural net. In the next trial, seventeen models with varying depths and locations for edge breaking defects were built. Only combination wave packets were used to interrogate the seventeen models since the use of only antisymmetric and symmetric Lamb waves did not gain us any extra information. Due to the fact that the FFT is a linear transformation describing the data, we decided not to perform FFT's on the data presented to the network.

NEURAL NETWORK TOPOLOGY

Since the initial trial to train the network for both defect characteristics at once had failed, it was decided to train a network to find the presence of a defect and then determine its length and finally the location using three different neural networks with the latter two being combined into one network after success of each individual

network. Different neural network logic schemes and topology of the hidden layers was tried for each of the three networks. Different networks were run to find the best network logic and topology for the final three networks. The results varied from 0.18 % error in the test value returned for a standard back-propagation network with one hidden layer of 50 processing elements to 86 % error for a cumulative back-propagation network with two hidden layers of twenty and ten processing elements respectively. Each trial was tested at certain time intervals to prevent over-training of the network from occurring. Success was achieved in training individual networks for each defect parameter and to detect the existence of a defect. The training data was combined and fed into a network that would determine both defect parameters at once. The final logic and topology used for the classification network which determined the existence of a defect was cumulative back propagation with twenty-four inputs and one hidden layer of twenty processing elements. Seventeen training data sets were used for this neural network. The network that determined length and location used standard back-ropagation with twenty-four inputs, two hidden layers of twenty and ten processing elements respectively. There were fifteen training data sets used for this network.

RESULTS

The first trials using the three different wave packets to interrogate the edge breaking defect were not successful as stated above, but allowed the observation of the sensitivity of the individual symmetric and antisymmetric Lamb waves to the defect parameters of length and in-plane location. The symmetric wave was sensitive to the variations in the in-plane location of the defect while the antisymmetric was not except for the case of a center line defect. The antisymmetric wave was sensitive to the length of the center line defect while the symmetric wave showed no response to varying length. This enabled us to better understand what the neural network would be looking for during the training but no quantitative conclusions could be made due to the lack of enough data sets and complexity of the wave forms.

Using the second set of edge breaking defect data with the previously mentioned configurations for the classification and characterization neural networks, good results were achieved after only training the networks for about thirty minutes each. They were stopped and tested at this point with test cases which were not in the training data sets. Further iteration could have been carried out, but the results were satisfactory for this initial study. For the classification network, a test case of no defect was tested. The network's returned yes/no value was within less than one percent using a 1.0 for a yes and a 0.0 for a no defect. For the length and length of edge breaking flaw network, two test cases were run. For the first test case, the network's returned value for the location and length of the defect which were respectively 0.01 and 5.8 % off from the actual value. In the second test case, the network's returned values which were 2 % for the location and 5.6 % off from the actual values for the length. This difference can be attributed to the network training longer on one test case than the other, and to not enough data sets describing the range in which the second test defect's parameters were located.

For the case of Lamb wave interaction with in-plane defects, only models which used either antisymmetric and symmetric Lamb waves interacting with defects of different lengths and locations were generated. Due to the problem discussed previously about combining these two signals to make another data set, there was not

enough data to train neural networks to find and quantify in-plane defects in order to make the publication deadline for this paper. The results of the models, however, allow us to make some qualitative comparisons about the sensitivity of each type of Lamb wave similar to those stated for the edge breaking defect. The symmetric wave shows variations due to change of the in-plane location of the defect while the anti-symmetric exhibits no change. On the other hand, the antisymmetric wave is sensitive to the length of the center line defect while the symmetric wave shows no variation for changes in length. Based on what was learned during the development of neural networks to find and characterize edge breaking defects, we feel confident that the same procedure will yield similar networks that can detect the presence and characteristics of length and in-plane location of a buried defect.

CONCLUSIONS

This paper has shown that using FE modeling to train neural networks to find and characterize edge breaking defects in rivet holes can be achieved with results better than 92%. This was accomplished using enough training data with two networks having different training logic and topology. Even though initial trials failed, the use of the individual wave packets to interogatte the two types of defects allowed us to better undestand the Lamb wave interaction with these defects. Initial findings for the in-plane buried defects were presented although networks had yet to be trained at the time of this publication. We anticipate that similar results will be obtained using the techniques developed for the edge breaking defect neural networks when applied to the in-plane defect cases.

ACKNOWLEDGEMENTS

This research was supported by the Texas Higher Education Coordinating Board under project number 1922.

REFERENCES

1. Schumacher, N. A., Verdict, G. S., Burger, C. P., and Gien, P. H., "An Experimental/FEM Study of Lamb Waves", Proc. 1991 Spring Conference Society for Experimental Mechanics, Milwaukee, Wisconsin, Proc. pp. 145-151 (June 1991).
2. Duffer, C. E., Verdict, G. S., Gien, P.H., and Burger, C. P.," Hybrid Experimental and Finite Element Studies of Rayleigh Wave Interaction with Shallow Surface Flaws for Depth Characterization," Proc. 1991 ASTM 23rd National Symposium On Fracture Mechanics, College Station, Texas, ASTM (June 1991).
3. Burger, C. P.,Smith, J. A., Dudderar, T. D., Gilbert, J. A., Peterson, B. R., "The Use of Fiber Optic Interferometry to Sense Ultrasonic Waves," ISA Transactions, Vol. 28(2), pp. 51-55 (1989).
4. Schumacher, N. A., Fiber Tip Interferometer for Non-Contact Ultrasonic NDE, M.S. Thesis, Texas A&M University, (August 1990).
5. Machiraju, R., Gien, P. H., Burger, C. P.,"Thermal wave generation: A nonlinear study of pulsed laser heating", Review of Progress in Quantitative NDE, Bowdoin College, Brunswick Maine, July 28, 1991.